the latter surrounded by six oxygen atoms arranged at the vertices of a distorted octahedron. One of the six O atoms is an atom from the bromite anion (see Figure 1), and the remainder are water molecules. The stoichiometry requires that some of the water molecules be associated with more than one octahedron, and zigzag chains of edge-linked octahedra are present in the solid. The compound is isomorphous with the corresponding chlorine compound,[22] and Br-O distances of 1.731 (2) and 1.702 (2) Å may be compared with Cl-O distances of 1.564 (1) and 1.557 (1) Å, The anion, as expected, is a bent species with a bond angle (O-Br-O = 105.3 (1)°) comparable with the O-Cl-O angle (108.23 (6)°) in $NaClO_2 \cdot 3H_2O$.[22] The Br-O distances in the oxoanions decrease with increasing bromine oxidation state, and the present values can be compared with the Br-O distances in $NaBrO_3$[23] (1.648 (4) Å) and $KBrO_4$[24] (1,59 (1)-1.62 (1) Å).

Bromine K-edge EXAFS data were obtained for solid $NaBrO_2 \cdot 3H_2O$ diluted with boron nitride and for saturated aqueous solutions. The k^3 weighted data obtained after background subtraction were used for curve fitting without smoothing or Fourier filtering, and the background-subtracted data and the corresponding Fourier transform for solid $NaBrO_2 \cdot 3H_2O$ are shown in Figure 2. The fitting employed the single scattering curved wave theory as contained in the EXCURVE program and utilized ab initio phase shifts calculated in the usual manner.[18] Analysis of the data from solid-state samples gave an average Br-O distance of 1.75 Å,[25] and no further shells arising from other neighboring atoms are statistically significant. In solution, a Br-O bond length of 1,72 Å[25] was obtained. Both values compare well with the bond lengths obtained from the X-ray study and suggest that EXAFS results for related compounds of uncertain structure may be viewed with confidence.

Acknowledgment. We thank the SERC for support, Dr. D. C. Povey of the University of Surrey for the X-ray data collection, the Director of the Daresbury Laboratory for the provision of facilities, and Dr. T. R. Gilson for collection of the Raman data,

Supplementary Material Available: Tables of anisotropic thermal parameters, bond lengths, and bond angles (2 pages); table of observed and calculated structure factors (6 pages). Ordering information is given on any current masthead page.

(22) Tarimci, C.; Schempp, E.; Chang, S. C. *Acta Crystallogr.* **1975**, *B31*, 2146-2149.
(23) Abrahams, S. C.; Bernstein, J. L. *Acta Crystallogr.* **1977**, *B33*, 3601-3604.
(24) Siegel, S.; Tani, B.; Appelman, E. *Inorg. Chem.* **1969**, *8*, 1190-1191.

(25) Systematic errors in data collection and analysis give rise to errors of ca. ±0.02-0.03 Å in the first shell distances. $NaBrO_2 \cdot 3H_2O$: $2\sigma^2 = 0.013$ Å, F1 = 0.04, R = 11.9. $NaBrO_2$ (aqueous solution): $2\sigma^2 = 0.009$ Å, F1 = 0.20, R = 11.4. F1 = $\sum_i (\chi_i^T - \chi_i^E)k_i^3$. $R = [\int|\chi^T - \chi^E|k^3\,dk / \int|\chi^E|\,dk] \times 100$.

Application of Molecular Dynamics and Free Energy Perturbation Methods to Metalloporphyrin-Ligand Systems. 1. CO and Dioxygen Binding to Four Heme Systems

Marco A. Lopez[‡] and Peter A. Kollman*

Contribution from the Department of Pharmaceutical Chemistry, University of California, San Francisco, San Francisco, California 94143. *Received July 28, 1988*

Abstract: We present the application of molecular mechanics/dynamics and free energy perturbation computational techniques to simulation of iron(II) porphyrin systems. Force field parameters were developed by modeling the geometry of four systems whose crystal structure is known, This force field was then used in molecular dynamics/free energy perturbation calculations, at 300 K in vacuo, on a separate set of four iron(II) porphyrin systems including models of 5,5-pyridine cyclophane heme(1,5-DCI) (I), picket fence heme(2-MeIm) (II), monochelated heme (III), and 7,7-durene cyclophane heme(1,5-DCI) (IV). The perturbation calculations reproduced reasonably well the trend in the partition coefficient, M value, of this set. Our simplified model indicates that the electrostatic component of both I and II favors the binding of O_2 over CO, whereas the electrostatic component of III and IV favors CO over O_2, The preference of O_2 over CO binding from the nonbonded steric component was I > II > III > IV. Molecular dynamics simulations showed that the Fe atom of the O_2 and CO complexes of I oscillated 0.06 and 0.16 Å, respectively, *lower* than those of II, even though the crystal structure and the simulation of the O_2 complex of II shows the Fe atom 0.087 Å *below* the porphyrin plane: this result suggests that the ratios of "R state" to "T state" CO/O_2 binding affinities will be extremely low for system I. The simulations also showed that even with a 7,7-strap as in IV, there is still more interaction with a bound CO than with a bound O_2.

Understanding the interaction of metalloproteins with substrates continues to be of interest.[1] The binding of small ligands to heme proteins has been extensively investigated with a variety of model systems.[2-6,9-13] These studies indicate that polarity and distal steric effects appear to dominate the discrimination between the binding of dioxygen and carbon monoxide to simple iron porphyrins. The relative binding of these two ligands to hemes and heme proteins is characterized in terms of the formal equilibrium shown in eq 1, where the $P^i_{1/2}$ is defined as the pressure of gas

$$HmO_2 + CO \overset{M}{\rightleftharpoons} HmCO + O_2 \qquad (1)$$

$$M = \frac{[HMCO][O_2]}{[HmO_2][CO]} = \frac{P^{O_2}{}_{1/2}}{P^{CO}{}_{1/2}}$$

i needed to saturate one-half of all hemes in solution and is the inverse of the binding constant of gas i. The partition coefficient,

[‡]Present address: Department of Chemistry and Biochemistry, California State University, Long Beach, Long Beach, CA 90840-3903.

(1) (a) Perutz, M. F. *Ann. Rev. Biochem.* **1979**, *48*, 327-86. (b) Tucker, P. W.; Phillips, S. E. V.; Perutz, M. F.; Houtchens, R.; Caughey, W. L. *Proc. Natl. Acad. Sci. U.S.A.* **1978**, *75*, 1076-1080. (c) Moffat, K.; Deatherage, J. F.; Seybert, D. W. *Science* **1979**, *206*, 1035-42. (d) Case, D. A.; Karplus, M. *J. Mol. Biol.* **1979**, *132*, 343-68.

0002-7863/89/1511-6212$01.50/0

M, varies in heme models from 50 000[3] to 5,[4] while in proteins the range is 6000 for *Glycera Hb*[7] to 0.075 for *Acaris Hb*.[8] (*Ascaris Hb* is the only heme model or heme protein that binds dioxygen with greater affinity than it binds CO.) It is easier to analyze the sources of the different factors affecting the partition coefficient in model systems than in proteins. Systems of the former have been synthesized where one structural feature is varied and the rest of the external factors kept constant. These systems include the "cyclophanes",[2b,4,9] "caps",[10] "straps",[11] "pocket",[2a] "basket",[2c,12] and "open"[5,6,13] systems. The sources of the different factors affecting the partition coefficient in proteins are much more difficult to analyze. Since all Hb's and Mb's have the same iron protoporphyrin IX prosthetic group,[14] the factors resulting in the wide range of heme protein partition coefficients must be due to the large number of interactions between the amino acid residues near the binding site.

The relative contributions due to different effects are not fully understood for even simple porphyrin models, much less for metalloproteins, and further study/development of heme proteins and heme protein model systems requires complete understanding of the different factors. The nature of experimental studies makes it very difficult to determine the relative factors and their importance in affecting the observed differences in the binding affinities of small ligands. Theoretical methods can be used to estimate the relative importance of different factors affecting these processes. Although accurate simulations of absolute CO versus dioxygen binding affinities require a full and accurate quantum mechanical treatment and are presently not possible for such large systems containing transition metals, the goal of this study is to compare different environmental effects on the relative affinity of these two ligands. Molecular mechanics/dynamics and free energy perturbation techniques appear to be well suited to look at the relative environmental effects on CO and dioxygen binding to model heme systems and to heme proteins.

In this paper we begin the study of heme model systems. The three goals in this study are (1) to develop force field parameters to reproduce structural properties of iron porphyrins, (2) to apply free energy perturbation theory and molecular dynamics to simulate environmental effects on the relative affinity of CO and O_2 in these systems, and (3) to analyze the molecular dynamics of porphyrin systems.

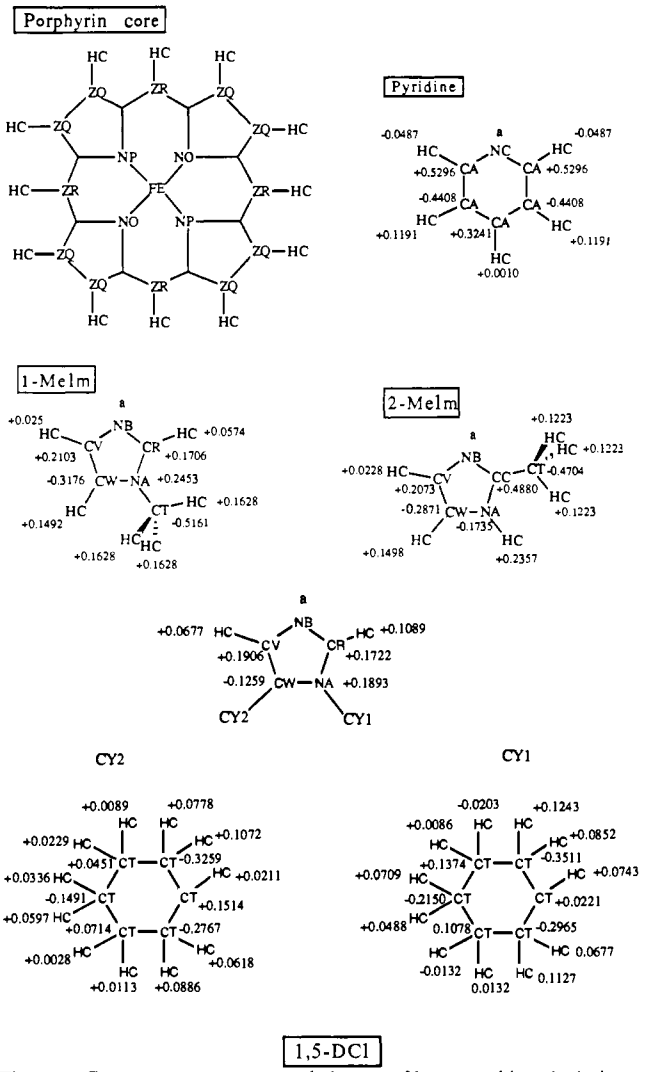

Figure 1. Structure, atom types, and charges of bases used in calculations and the atom types of atoms in the porphyrin cores (see Table I for porphyrin core charges). (a) See Scheme I for charge.

Scheme I

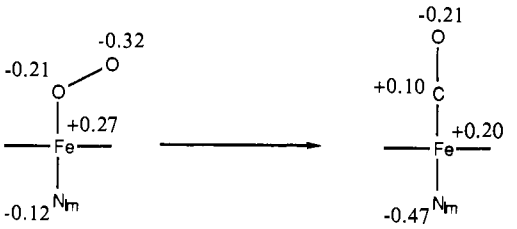

Methods

All the present work was done in the context of the AMBER[15] software package. The basic equation of the force field is given in eq 2. Calculations were done using a constant dielectric, $\epsilon = 1$. A VAX 8650 or

$$E_{total} = \sum_{bonds} K_r(r - r_{eq})^2 + \sum_{angles} K_\theta(\theta - \theta_{eq})^2 + \sum_{dihedrals} \frac{V_n}{2}[1 + \cos(n\phi - \gamma)] + \sum_{i<j} \left[\frac{A_{ij}}{R_{ij}^{12}} - \frac{B_{ij}}{R_{ij}^{6}} + \frac{q_i q_j}{\epsilon R_{ij}}\right] + \sum_{H\ bonds} \left[\frac{C_{ij}}{R_{ij}^{12}} - \frac{D_{ij}}{R_{ij}^{10}}\right] \quad (2)$$

(2) (a) Collman, J. P.; Brauman, J. I.; Iverson, B. L.; Sessler, J. L.; Morris, R. M.; Gibson, Q. H. *J. Am. Chem. Soc.* **1983**, *105*, 3052. (b) Traylor, T. G.; Tsuchiya, S.; Campbell, D.; Mitchell, M.; Stynes, D.; Koga, N. *J. Am. Chem. Soc.* **1985**, *107*, 604–14. (c) Momenteau, M.; Scheidt, W. R.; Eigenbrot, C. W.; Reed, C. A. *Ibid.* **1988**, *110*, 1207–1215.

(3) David, S.; Dolphin, D.; James, B. R. In *Frontiers in Bioinorganic Chemistry*; Xavier, A. V., Ed.; VCH: New York, 1986; pp 163–182, and references therein.

(4) Traylor, T. G.; Koga, N.; Deardurff, L. A. *J. Am. Chem. Soc.* **1985**, *107*, 6504–10, and references therein.

(5) Jameson, G. B.; Molinaro, F. S.; Ibers, J. A.; Collman, J. P.; Brauman, J. I.; Rose, E.; Suslick, K. S. *J. Am. Chem. Soc.* **1980**, *102*, 3224–37.

(6) Chang, C. K.; Traylor, T. G. *Proc. Natl. Acad. Sci. U.S.A.* **1973**, *70*, 2647.

(7) Parkhurst, L. J.; Sima, P.; Goss, D. J. *Biochemistry* **1980**, *19*, 2688–92.

(8) Gibson, Q. H.; Smith, M. H. *Proc. R. Soc. London, Ser. B* **1965**, *163*, 206–14.

(9) Traylor, T. G.; Koga, N.; Deardurff, L. A.; Swepston, P. N.; Ibers, J. A. *J. Am. Chem. Soc.* **1984**, *106*, 5132.

(10) (a) Shimizu, M.; Basolo, F.; Vallejo, M. N.; Baldwin, J. E. *Inorg. Chim. Acta* **1984**, *91*, 247. (b) Rose, E. J.; Basolo, F.; Venkatasubramanian, P. N.; Swartz, J. C.; Jones, R. D.; Hoffman, B. M. *Proc. Natl. Acad. Sci. U.S.A.* **1982**, *79*, 5742.

(11) Ward, B.; Wang, C.-B.; Chang, C. K. *J. Am. Chem. Soc.* **1981**, *103*, 5236.

(12) Collman, J. P.; Brauman, J. I.; Fitzgerald, J. P.; Sparapany, J. W.; Ibers, J. A. *J. Am. Chem. Soc.* **1988**, *110*, 3486.

(13) Jameson, G. B.; Rodley, G. A.; Robinson, W. T.; Gagne, R. R.; Reed, C. A.; Collman, J. P. *Inorg. Chem.* **1978**, *4*, 850–7.

(14) (a) Bunn, H. T.; Forget, B. G.; Franklin, H. *Human Hemoglobins*; W. B. Saunders: Philadelphia, 1987. (b) Kagen, L. J. *Myoglobin-Biochemical, Physiological and Clinical Aspects*; Columbia University Press: New York, 1973; pp 9–39.

(15) (a) Weiner, P. K.; Kollman, P. A. *J. Comput. Chem.* **1981**, *2*, 287–303. (b) Weiner, S. J.; Kollman, P. A.; Case, D. A.; Singh, U. C.; Ghio, C.; Alagona, G.; Profeta, S.; Wiener, P. *J. Am. Chem. Soc.* **1984**, *106*, 765–784. (c) Weiner, S. J.; Kollman, P. A.; Nguyen, D. T.; Case, D. A. *J. Comput. Chem.* **1986**, *7*, 230–252. (d) Singh, U. C.; Weiner, P. K.; Caldwell, J.; Kollman, P. A. AMBER 3.0, University of California—San Francisco, 1987.

Table I. Atom Types, Symmetry Labels, and Charges of the Porphyrin Core[a]

atom types	sym label	charge
NP(O)	N_{pyr}	-0.1800
CC	C_α	+0.0250
ZQ	C_β	-0.0075
ZR	C_m	+0.0401
HC		+0.0212[b]
FE		c

[a] See Figure 1. [b] This value was used for the picket fence, 5,5-pyridine, and 7,7-durene systems. To ensure charge neutrality, each of the following systems had a different charge: flat heme and model a, +0.0239; model b, +0.0125; model c, +0.0217; model d, +0.0122. [c] See Scheme I.

an FPS 264 computer was used to do these calculations. Starting values for the bond, angle, dihedral, and van der Waals parameters were supplied by D. Case,[16] taken from—or developed by analogy with—those given by Weiner et al.[15b,c] The atom types used for the bound sixth ligands were FE-O3-OT and Fe-Z-OT, for Fe-O_2 and Fe-CO, respectively. For all systems, the Fe atom was grouped with the proximal base to form one residue, the atoms of the porphyrin core formed a second residue, and the O_2 or CO ligands formed a third. For the picket fence system each phenylpivalamido "picket" formed a separate residue. For the 5,5-pyridine and 7,7-durene systems, the straps were composed of three residues, two from the linking atoms and the third from the cap.

Charges. The charges used for the porphyrin core and its O_2 and CO ligands were calculated at the IEHT level.[16] The partial charges of the bases, "straps", and "pickets" of the heme systems were obtained—at the STO3G level following AM1[17] geometry optimization—via the program GAUSSIAN 80 UCSF[18] using the fitting procedure described previously.[19] The partial charges of the 5,5-pyridine and 7,7-durene straps were determined by calculating the charge distribution of 2-azapentanoic acid and 3,5-dihydropyridine for the 5,5-pyridine strap and of 1,7-dihydroheptane and 1,4-dihydro-2,3,5,6-tetramethylbenzene for the 7,7-durene strap. The partial charges of the phenylpivalamide "pickets" were taken from those calculated for phenylacetamide.

For all systems studied the partial charges of the nitrogen atom of the proximal base, the iron atom, and both atoms of the CO and O_2 ligands were those shown in Scheme I. To maintain charge neutrality, excess partial charge was distributed equally to the protons of the porphyrin core. The structures and charges of the porphyrin core and of the proximal bases used in this study are given in Figure 1 and Table I.

Force Field Development

The molecular mechanical parameters for the heme models were developed by simulating the stereochemistry around the iron atom in four heme complexes whose X-ray crystal structures are known. These four systems are the following: (a) "picket fence" (1-MeIm)(O_2) [(1-methylimidazole)-*meso*-[tetrakis($\alpha,\alpha,\alpha,\alpha$-*o*-pivalamidophenyl)porphyrinato]iron(II)(O_2)[13]]; (b) picket fence (2-MeIm);[13] (c) picket fence (2-MeIm)(O_2);[5] (d) pyridine-TPP-CO [(pyridine)-*meso*-[tetrakis($\alpha,\alpha,\alpha,\alpha$-phenyl)-porphyrinato]iron(II) (CO)[20]].

The quality of fit between calculated and known structures was assessed on the basis of the agreement between specific geometric features. These features included the following: (a) the direction and extent of the displacement of the iron atom from the planes defined by the four pyrrole nitrogens (Fe-Ct) and all of the 24 atoms of the porphyrin core (Fe-core); (b) the iron-proximal nitrogen bond distance (FE-NB); (c) the bond distance between the iron atom and the sixth ligand (Fe-L1); (d) the average iron-pyrrole nitrogen bond length (Fe-Np); (e) the size of the pyrrole-nitrogen "hole" (Ct-Np); (f) the N_{pyr}-Fe-N_{pyr} bond angles; (g) the extent of "pyrrole-tilting" (Ct_β-Ct). This last feature is determined in two ways: (1) There are four sets of symmetry-related atoms in the porphyrin core; the four pyrrole

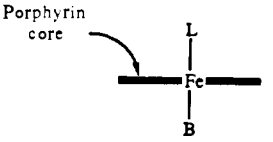

Model	L	B
a	O_2	1-MeIm
b		2-MeIm
c	O_2	2-MeIm
d	CO	pyridine

Figure 2. Structures of models used in the force field development; porphyrin core and bases are shown in Figure 1. The hydrogens shown attached to the four meso carbons (ZR) were left off in models a–d.

nitrogens, N_{pyr}, the four meso carbons, C_m, the eight α-pyrrole carbons, C_α, and the eight β-pyrrole carbons, C_β. Each of these four groups can be considered to form a "circle" with its own "center" and "radius". The amount of "pyrrole-tilting" can be evaluated by the computing the difference between the "centers" of the pyrrole-nitrogen "circle" (Ct_N) and the β-carbon "circle" (Ct_β). If there is no tilting, the difference between these two centers is zero. As the tilting increases, these two centers move further and further apart. (2) A second way of determining the extent of "pyrrole-tilting" is to examine the C_α-C_m-C_α-N_p dihedral angle. However, the values of these dihedral angles are dependent on the movement of two pyrrole groups and as such are not as accurate a determination of the pyrrole tilting.

For the parameter adjustments, all four of the models referred to below (a–d) used the simplified porphyrin systems shown in Figure 2.

The first model whose structural properties were modeled was b, in particular, its displacement of iron from the porphyrin plane. The displacement of this iron atom was found to be independent of starting geometry. Initial structures where the iron was both above and below the porphyrin plane resulted in the same minimized structure.

The problem of defining θ_{eq}(N_{pyr}-Fe-N_{pyr}) for both dimetrically opposed pyrrole-nitrogen pairs (180°) and orthogonally oriented pyrrole-nitrogen pairs (90°) was overcome by defining two pyrrole nitrogen atom types, NP and NO.[16] All force field parameters for these two are the same except for θ_{eq}(NP-Fe-NP), θ_{eq}(NO-Fe-NO), both 180°, and θ_{eq}(NP-Fe-NO), 90°. The r_{eq}(Fe-NP(O)) and r_{eq}(Fe-NB) values were adjusted so as to yield the correct displacement of iron in model b. As the r_{eq}(Fe-NB) was decreased (2.10 → 2.07 Å), the Fe-Ct distance of the minimized structure increased (0.307 → 0.336 Å). Increasing the K_r of the Fe-NP(O) (30.0 → 50.0 kcal/rad^2) also increased the Fe-Ct displacement (0.336 → 0.404 Å). This last adjustment increased the Fe-Np distance (2.062 → 2.077 Å). The parameters were left at 2.10 Å and 50.0 kcal/Å^2 for Fe-NP(O) and 2.07 Å and 50.0 kcal/Å^2 for Fe-NB.

The force field was then used to reproduce the structural properties of model a. The number of properties that were followed was expanded to include the pyrrole-nitrogen "hole", Ct-Np, the ligand-iron bond length, Fe-L1, and the Fe-L1-O, N_{pyr}-Fe-N_{pyr}, and L1-Fe-N_{pyr} bond angles. The force field gave Fe-Np lengths that were too long (2.041 Å), a Ct-Np length that was too large (2.041 Å), but an Fe-Ct length that was correct. The r_{eq}(Fe-NP(O)) value was varied (2.06 → 2.08 → 2.10 Å), and all the properties listed were followed for both a and b, The value of 2.10 Å gave correct Fe-Np and Ct-Fe lengths and N_{pyr}-Fe-N_{pyr} angle for b. However, the Fe-Np distance for a was too long (2.041 Å) and the Ct-Np length was too large (2.041 Å). It appeared that by switching the system from b to a the force field caused the Fe to be pulled back into the plane and caused the porphyrin to "open up", that is, the C_α-C_m-C_α angle increased and the C_β-C_α-N_{pyr} angle decreased as the Fe was brought back into the plane. To counteract this tendency, the θ_{eq}(C_α-C_m-C_α) value was decreased (124 → 115°) and the θ_{eq}(C_β-C_α-N_{pyr}) value was increased (110.3 → 114.0°). In addition the r_{eq}(Fe-NB) value was increased (2.07 → 2.08 Å) and the r_{eq}(Fe-NP(O)) was made shorter (2.10 → 2.06 Å). These adjustments left the minimized a values in good agreement with experiment. The Fe-Np and Ct-Np distances were perfect. The other properties were within 1° or 0.02 Å. The values corresponding to model b were also very

(16) D. Case supplied the appropriate parameters from Giammona, D. A. Ph.D. Dissertation, University of California, Davis, 1986.
(17) (a) Dewar, M. J. S.; Zoebisch, E. G.; Healy, E. F.; Stewart, J. J. P. *J. Am. Chem. Soc.* **1985**, *107*, 3902–9. (b) Dewar, M. J. S.; Dieter, K. M. *J. Am. Chem. Soc.* **1986**, *108*, 8075–86.
(18) Singh, U. C.; Kollman, P. A. GAUSSIAN 80 UCSF. *Quantum Chemistry Exchange Program Bull.* **1982**, *2*, 17.
(19) Singh, U. C.; Kollman, P. A. *J. Comput. Chem.* **1984**, *5*, 129–145.
(20) Peng, S. M.; Ibers, J. A. *J. Am. Chem. Soc.* **1976**, *98*, 8032–6.

Table II. Values of Specific Geometrical Features for Four Simulated Heme Model Systems[a] and Known Structures (Distances in angstroms)

feature[b]	O_2-1-MeIm (a)	2-MeIm (b)	O_2-2-MeIm (c)	CO-pyridine (d)
Fe-Ct	+0.025 (+0.030)	-0.353 (-0.399)	-0.057 (-0.087)	+0.022 (+0.024)
Fe-core	-0.008 (+0.016)	-0.387 (-0.425)	-0.117 (-0.112)	+0.009 (0.000)
Ct_β-Ct	0.057 (0.034)	0.059 (0.070)	0.106 (0.063)	0.053 (0.036)
Ct-Np	2.027 (1.987)	2.018 (2.033)	2.027 (1.994)	2.027 (2.017)
Fe-Np	2.027 (1.987)	2.048 (2.072)	2.028 (1.996)	2.028 (2.017)
Fe-NB	2.052 (2.069)	2.068 (2.095)	2.133 (2.107)	2.133 (2.107)
Fe-Ll	1.799 (1.746)		1.805 (1.898)	1.774 (1.769)

[a] Symbols used: 1-MeIm = 1-methylimidazole, 2-MeIm = 2-methylimidazole, + = the displacement of the iron is toward the distal side of the heme, - = the displacement of the iron is toward the proximal side of the heme. [b] See text for definitions.

close to those of the known structure except for the values of Fe-Np and Ct-Np. They were both too small by 0.06 Å. A further adjustment to correct this was to allow the porphyrin ring to "relax" by simultaneously increasing the $\theta_{eq}(C_\alpha-C_m-C_\alpha)$ value (114 → 118°), decreasing the $\theta_{eq}(C_\beta-C_\alpha-N_{pyr})$ value (114 → 112°), and lengthening the r_{eq}(Fe-NP(O)) value (2.06 → 2.09 Å). Furthermore, the r_{eq}(Fe-NB) value was increased (2.08 → 2.09 Å). These adjustments cut both the Fe-Np and Ct-Np discrepancies from 0.06 to 0.03 Å and left the corresponding values of model a both 0.02 Å too large. This was the state of the force field before applying it to reproduce the geometry of model c.

The force field was used to generate a minimized structure corresponding to model c. Comparison with the known structure showed excellent agreement between the two. The differences in distance parameters followed so far were all ≤0.025 Å, and the angle parameters were all ≤1°. The Fe-O-O angle was 2.3° off, so the θ_{eq}(Fe-O3-OT) value was increased (129.0 → 130.0°). The r_{eq}(Fe-O3) value was decreased (1.85 → 1.80 Å). After these last ajustments, the force field reproduced the structural properties of the three models a, b and c quite well.

Next, the force field was used to construct model d. This model has pyridine as the proximal base. The AMBER atom type NC is used for the pyridine nitrogen. The r_{eq}(Fe-NC) parameter is treated the same as r_{eq}(Fe-NB) in the present force field. Comparison with the published crystal structure showed good agreement for all distances and angles except for the displacement of the iron from the porphyrin. The value found in the crystal structure was 0.024 Å *toward the CO* (+) while the calculated structure showed a displacement of 0.086 Å *toward the base* (-). This problem was corrected for the CO structure by decreasing the $\theta_{eq}(Z-Fe-N_{pyr})$ value (100 → 94.6°). The same problem, the direction of displacement of the Fe atom from the porphyrin, was also present in the O_2 complexes. The $\theta_{eq}(N_{pyr}-Fe-O3)$ value was increased (90.0 → 92.6°) to displace the Fe atom in the right direction. The position of the iron atom, in the three models that have a sixth ligand, is very sensitive to this $\theta_{eq}(N_{pyr}-Fe-L1)$ angle, and the adjustments thereof greatly improved the relative positions of the iron atom.

The only large discrepancy left was that the calculated structures were still "doming" ~0.1 Å too much. ["Doming" is used to describe the difference between the two planes defined by (a) the four pyrrole nitrogens and (b) all 24 heavy atoms of the porphyrin core.] Modifying the $X-C_\alpha-C_m-X$ torsion improved the "doming" effect a little but caused the Fe-Ct distance to be left too far away from the proximal side. The solution to this doming problem was to increase the $X-N_{pyr}-C_\alpha-X$ *general* dihedral torsion by 4× and relax the $Fe-N_{pyr}-C_\alpha-C_m$ and $Fe-N_{pyr}-C_\alpha-C_\beta$ *specific* dihedral torsions to 0. This last adjustment associated all the torsional rigidity of the porphyrin 24-atom structure to the rings but allowed the Fe atom great flexibility in motion directed along the normal to the porphyrin. Following the dihedral torsion adjustments, other parameters had to be readjusted. These final readjustments included decreasing $\theta_{eq}(C_\beta-C_\alpha-N_{pyr})$ (112 → 109°), decreasing $r_{eq}(Fe-N_{pyr})$ (2.09 → 2.06 Å), increasing $\theta_{eq}(C_\alpha-C_m-C_\alpha)$ (118 → 121°), increasing r_{eq}(Fe-O3) (1.80 → 1.82 Å), decreasing r_{eq}(Fe-NB) (2.09 → 2.05 Å), decreasing θ_{eq}(NP(O)-Fe-Z) (94.6 → 93.5°), and decreasing θ_{eq}(NP(O)-Fe-O3) (92.6 → 91.5°). The final values of the geometric features for the four calculated models are listed in Table II together with the corresponding values calculated with the coordinates of the reported crystal structures. The final set of force field parameters are listed in Table III.

Table III. Heme Force Field Parameters

bond	K_r, kcal mol^{-1} Å^{-2}	r_{eq}, Å	
FE-NO	50.0	2.06	
FE-NP	50.0	2.06	
FE-O3	50.0	1.86	
FE-NB	50.0	2.05	
FE-NC	50.0	2.05	
angle	**K_θ, kcal mol^{-1} rad^{-2}**	**θ_{eq}, deg**	
NP-CC-ZQ	70.0	109.0	
NO-CC-ZQ	70.0	109.0	
NP-FE-NP	0.0	179.9	
NP-FE-NO	0.0	90.0	
NP-FE-NB	0.0	90.0	
NO-FE-NB	0.0	90.0	
NP-FE-O3	50.0	91.5	
NO-FE-O3	50.0	91.5	
NO-FE-Z	50.0	93.5	
NP-FE-Z	50.0	93.5	
FE-O3-OT	70.0	130.0	
FE-Z-OT	70.0	179.9	
CC-ZR-CC	70.0	121.0	
dihedral	**V_n**	**2**	**γ**
X-NP-CC-X	22.80	180.0	2
X-NO-CC-X	22.80	180.0	2
FE-NP-CC-ZQ	0.0	180.0	2
FE-NO-CC-ZQ	0.0	180.0	2
FE-NO-CC-ZR	0.0	180.0	2
FE-NP-CC-ZR	0.0	180.0	2
vdW	**R^*, Å**	**ϵ, kcal mol^{-1}**	
FE	1.0	0.1	

Free Energy Perturbation Calculations

A very useful property of these calculational techniques is that they allow for the calculation of the *free energy* difference between two *similar* structures. The statistical perturbation theory has been presented elsewhere.[21,22] The perturbation calculations are done within the context of the following thermodynamic cycles:

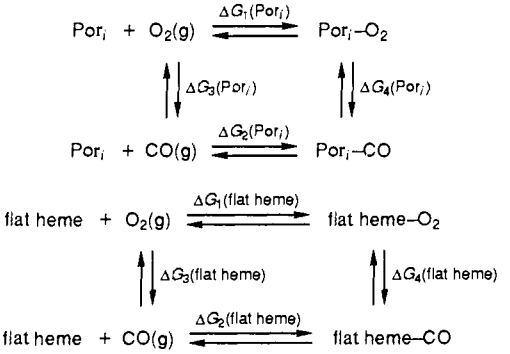

The quantities $\Delta G_1(Por_i)$ and $\Delta G_2(Por_i)$ have been experimentally

(21) Singh, U. C.; Brown, F. K.; Bash, P. A.; Kollman, P. A. *J. Am. Chem. Soc.* **1987**, *109*, 1607-14.
(22) Van Gunsteren, W. F. *Protein Eng.* **1988**, *1*, 5-13.

Table IV. Calculated and Experimental Gibbs Free Energy Differences for Four Heme Systems

	5,5-pyridine heme	picket fence heme	flat heme	7,7-durene heme
$\Delta G_4(\mathrm{Por}_i)$	4.1 ± 0.1	5.2 ± 0.1	−1.51 ± 0.044	−2.83 ± 0.04
exptl[a]	-1.56_4	-4.94_4	-5.91_4	-6.38_3
$\Delta\Delta G$(calcd)[b]	5.6 ± 0.4	6.7 ± 0.7	0	−1.3 ± 0.1
$\Delta\Delta G$(exptl)[c]	4.35	0.97	0	−0.47

[a] Values = $-RT$ ln (M) at 20–25 °C. [b] $\Delta\Delta G$(calcd) = $\Delta\Delta G_4(\mathrm{Por}_i)$ − $\Delta\Delta G_4$(flat heme). [c] $\Delta\Delta G$(exptl) = $[-RT \ln (M_{\mathrm{Por}_i}]$ − $[-RT \ln (M_{\text{flat heme}})]$.

determined for four representative systems (vide infra). Because these are thermodynamic cycles, the quantity $\Delta G_2(\mathrm{Por}_i) - \Delta G_1(\mathrm{Por}_i)$ is equal to the quantity $\Delta G_4(\mathrm{Por}_i) - \Delta G_3(\mathrm{Por}_i)$. The comparison of the calculated values with the experimental values will be through the differences between the free energy of the ith system and that of the reference system, flat heme, $\Delta\Delta G$(calcd), and $\Delta\Delta G$(exptl), respectively:

$$[\Delta G_4(\mathrm{Por}_i) - \Delta G_3(\mathrm{Por}_i)] - [\Delta G_4(\text{flat heme}) - \Delta G_3(\text{flat heme})] = [\Delta G_2(\mathrm{Por}_i) - \Delta G_1(\mathrm{Por}_i)] - [\Delta G_2(\text{flat heme}) - \Delta G_1(\text{flat heme})] \quad (3)$$

Since $\Delta G_3(\mathrm{Por}_i) = \Delta G_3$(flat heme) (both are the transformation of $O_2(g) \rightarrow CO(g)$) and $\Delta G_2(i) - \Delta G_1(i) = -RT \ln (M_i)$, eq 3 reduces to

$$\Delta G_4(\mathrm{Por}_i) - \Delta G_4(\text{flat heme}) = [-RT \ln (M_i)] - [-RT \ln (M_{\text{flat heme}})]$$

$$\Delta\Delta G(\text{calcd})_i = \Delta\Delta G(\text{exptl})_i \quad (4)$$

The quantity $\Delta G_4(\mathrm{Por}_i)$—although physically unrealizable—is straightforward to calculate;[21] it is given by eq 5, where $H_{CO}(\mathbf{r})$

$$\Delta G_4(\mathrm{Por}_i) = \sum_{j=1}^{20} -RT \ln \langle e^{-H_p(\mathbf{r},\lambda_j)/RT} \rangle \quad (5a)$$

$$H_p(\mathbf{r},\lambda_j) = \lambda_j H_{O_2}(\mathbf{r}) + (1 - \lambda_j) H_{CO}(\mathbf{r}) \quad (5b)$$

and $H_{O_2}(\mathbf{r})$ are the Hamiltonians of the Por–CO and Por–O_2 systems (given by eq 1), respectively, and the angular brackets denote an ensemble average. Starting with $H_{O_2}(\mathbf{r})$, the system is perturbed toward $H_{CO}(\mathbf{r})$ in 20 steps. At each step the force field is incremented, followed by 500 steps of molecular dynamics (MD) equilibration. Following this, the time averages[23] are collected over a second set of 500 MD steps. The value of $\Delta G_4(\mathrm{Por}_i)$ is given by the sum of these 20 steps.

The force field (vide supra) was used in such O_2-to-CO free energy perturbation calculations on four representative six-coordinate heme systems whose O_2/CO relative binding affinity is known. These calculations model this—in vacuo—relative binding affinity of two "distal-side strapped" systems (5,5-pyridine cyclophane heme[4] and 7,7-durene cyclophane heme,[3] both with the proximal base 1,5-dicyclohexylimidazole), "picket fence" heme, with 2-MeIm, and monochelated protoheme,[6] where the base is a 4-substituted imidazole (flat heme). The charges used for all the four systems are shown in Figures 1 and 3. In all the perturbation calculations, the charges of the iron atom, the two sixth-ligand atoms, and the nitrogen atom of the proximal base were perturbed in the way shown in Scheme I.[24] Stereoscopic views of the dioxygen complexes ($\lambda = 1$) of the four systems used in the perturbation calculations are shown in Figure 4. The results of the free energy perturbation calculations, for the four heme systems, are listed in Table IV together with the corresponding experimental values. In Table V are listed the estimates to the different components of the corresponding free energy values listed in Table IV. These estimates are calculated simultaneously with the calculation of ΔG_4 and are given by eq 6, where $H_p(\lambda)$ is the

$$\Delta G_4 = \sum_{\lambda} H_p(\lambda) \quad (6)$$

(23) According to the ergodic hypothesis ensemble averages may be replaced by time averages, see ref 27.

(24) Loew, G. H. In *Iron Porphyrins*; Lever, A. B. P., Gray, H. B., Eds.; Addison-Wesley: Reading, MA, 1983; Part 1, pp 1–88.

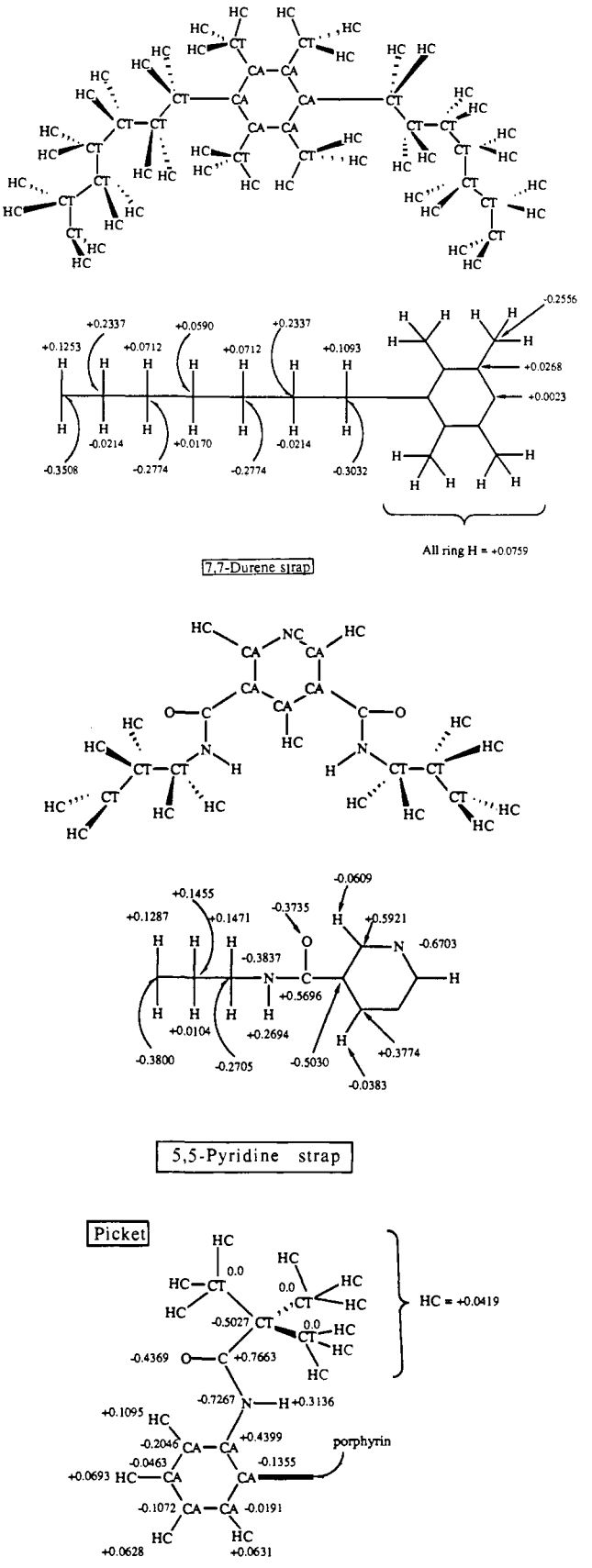

Figure 3. Structures, atom types, and charges of the heme systems used in the perturbation calculations; porphyrin cores are shown in Figure 1. The "picket fence" system is constructed by substituting a "picket" for the hydrogen at each of the four C_m (ZR) positions. The 5,5-pyridine and 7,7-durene systems are constructed by substituting the appropriate strap for two hydrogens at two diametrically opposed C_β (ZQ) positions. The flat heme system is the same as model a, Figure 2, with the addition of hydrogens at the four C_m positions.

Table V. Estimates of Various Contributions to the Calculated Free Energies, $\Delta\Delta G_4$, Listed in Table IV

component	5,5-pyridine heme	picket fence heme	flat heme	7,7-durene heme
EEL[a]	7.0 ± 0.1	8.6 ± 0.1	2.56 ± 0.03	1.27 ± 0.08
NONB[b]	0.73 ± 0.04	0.006 ± 0.030	−0.033 ± 0.001	−0.112 ± 0.004
14NB[c]	0.389 ± 0.005	0.27 ± 0.01	0.22 ± 0.01	0.202 ± 0.001
14EL[d]	−4.375 ± 0.002	−4.36 ± 0.01	−4.506 ± 0.006	−4.41 ± 0.01
BADH[e]	0.57 ± 0.03	1.00 ± 0.04	0.41 ± 0.04	0.24 ± 0.01
total elec[f]	2.7 ± 0.7	4.2 ± 0.9	−1.94 ± 0.08	−3.1 ± 0.1
total NElec[g]	1,69 ± 0.03	1.28 ± 0.04	0.60 ± 0.02	0.334 ± 0.003

[a] Electrostatic energy summed over all pairs connected by more than three bonds. [b] van der Waals energy summed over all pairs connected by more than three bonds. [c] van der Waals energy summed over all pairs connected by three bonds. [d] Electrostatic energy summed over all pairs connected by three bonds. [e] Potential energy contribution of all bonds, angles, and dihedral angles that involve some or all of the mutated atoms and at least one atom from a residue that contains no mutating atoms. [f] Sum of EEL and 14NB. [g] Sum of NONB, 14NB, and BADH.

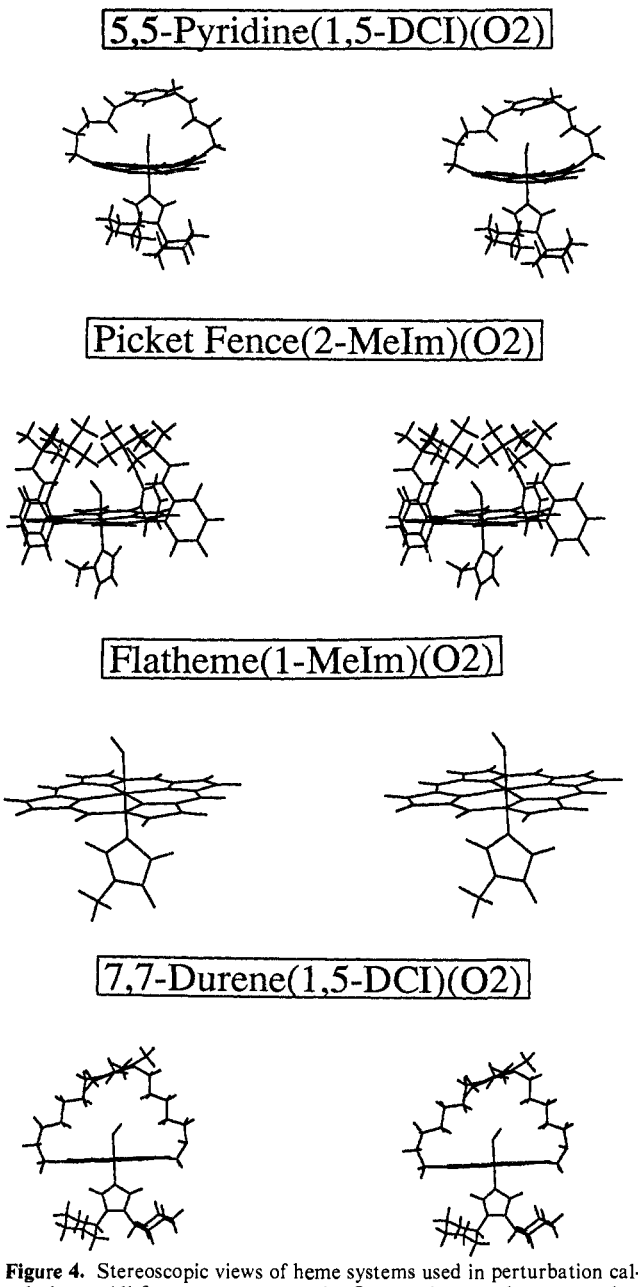

Figure 4. Stereoscopic views of heme systems used in perturbation calculations. All four structures are the O_2 complexes and correspond to the $\lambda = 0$ state.

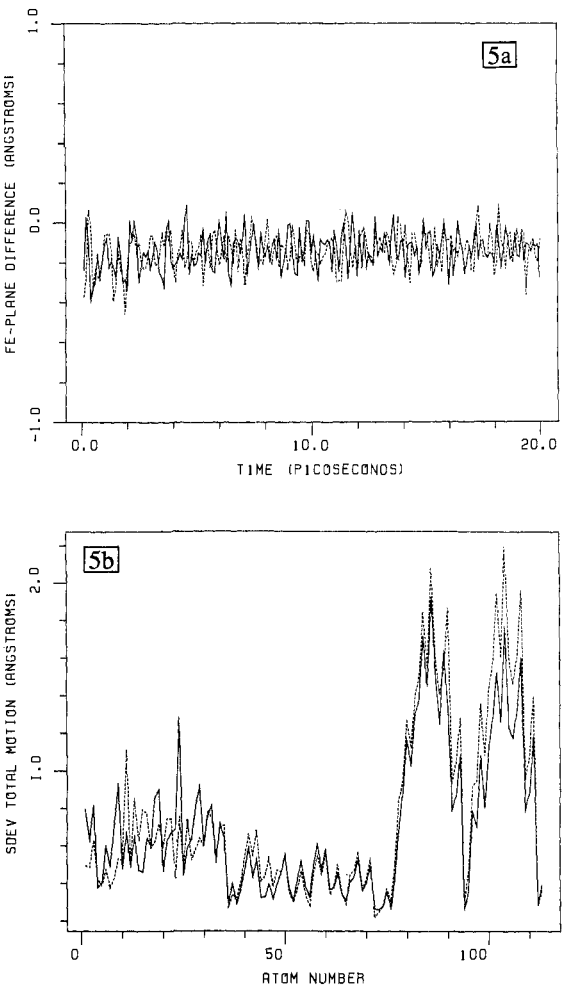

Figure 5. Plots obtained from the MD trajectories of the 5,5-pyridine system: (—) O_2 complex, (– –) CO complex. (a) The Fe–plane distance over 20 ps. (b) The total motion of the individual atoms; Atom numbers 1–35 are the pyridine cap and linking atoms; 36 and 37 are the O_2 or CO ligand; 38–71 are the porphyrin core; 72 is the Fe atom; 73–113 are the 1,5-DCI. Trajectories were collected every 0.1 ps over a total of 20 ps, at 300 K.

average Hamiltonian of the configurations generated during the second set of 500 MD steps (vide supra),

All the free energy perturbation calculations reported here are the result of at least two determinations: (a) Starting with the O_2 structure, $\lambda = 1$, and perturbing *to the CO complex*, $\lambda = 0$; (b) starting with this CO complex and perturbing *back to the O_2 complex*. The errors reported in Tables IV and V are the standard deviations from the results of these two calculations,

Molecular Dynamics

The eight representative systems (four CO complexes and four O_2 complexes) were run for 20 ps of molecular dynamics each, and trajectories were recorded every 0.1 ps. These were run in vacuo at 300 K by using 0.001-ps time steps. Shown in Figures 5–8 are four sets of plots from these trajectories. Each set consists of the following: (a) the Fe–plane (distance from Fe to the best-fitting 24-atom plane) distances over 20 ps; (b) the standard deviation of the total motion of each atom over the same 20 ps, Trajectories from both the O_2 and CO complexes are shown in

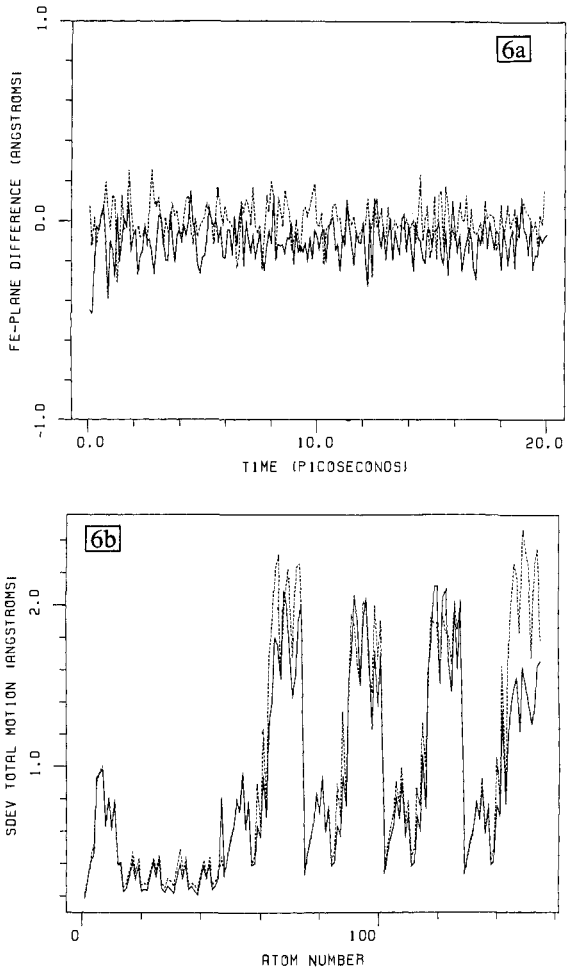

Figure 6. Plots obtained from the MD trajectories of the "picket fence" system: (—) O_2 complex; (---) CO complex. (a) The Fe–plane distance over 20 ps. (b) The total motion of the individual atoms: Atom number 1 is the Fe atom; 2–13 are the 2–methylimidazole; 14–45 are the porphyrin core; 46 and 47 are the O_2 or CO ligand; 48–74 are "picket 1"; 75–101 are "picket 2"; 102–128 are "picket 3"; 129–155 are "picket 4". Trajectories were collected every 0.1 ps over a total of 20 ps, at 300 K.

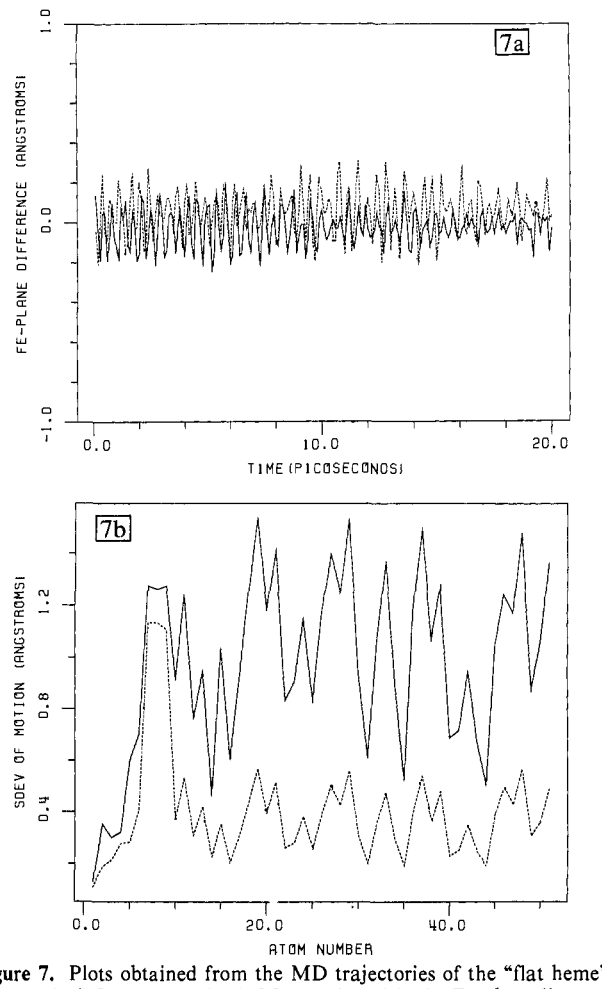

Figure 7. Plots obtained from the MD trajectories of the "flat heme" system: (—) O_2 complex; (---) CO complex. (a) The Fe–plane distance over 20 ps. (b) The total motion of the individual atoms. Atom number 1 is the Fe atom; 2–13 are the 1-methylimidazole; 14 and 15 are the O_2 or CO ligand; 16–51 are the porphyrin core. Trajectories were collected every 0.1 ps over a total of 20 ps, at 300 K.

Table VI. Values of Specific Geometrical Features for the Picket Fence(2-MeIm)(O_2) System from Four Sources

feature[e]	X-ray[a]	min[b]	MD-rms[c]	MD-av[d]
Fe–Ct	−0.087	−0.074	−0.072	−0.086 ± 0.094
Fe–core	−0.112	−0.131	−0.093	−0.107 ± 0.110
Ct_β–Ct	0.063	0.110	0.040	0.085 ± 0.052
Ct–Np	1.994	2.026	2.019	2.025 ± 0.022
Fe–Np	1.996	2.027	2.020	2.028 ± 0.023
Fe–NB	2.107	2.127	2.147	2.169 ± 0.076
Fe–L1	1.898	1.795	1.818	1.829 ± 0.079

[a] See ref 5. [b] Structure obtained after running the X-ray structure geometry through ~2000 steps of conjugate gradient minimization. [c] Parameters calculated for the average structure from the trajectories recorded over 20 ps. [d] Values are the mean and standard deviation of values from each of the 200 sets of the MD trajectory. [e] See text for definitions.

each figure. In Table VI are listed the same geometrical features that were used in deriving the force field and values for each for the picket fence (O_2) system from four sources: (1) the X-ray structure;[5] (2) the minimized structure that served as the origin for the MD trajectories; (3) the average structure obtained from the MD trajectories; (4) the averaged values of the structural parameters from each of the 200 coordinate sets in the trajectory. The amount of "tilting" undergone by each of the four pyrroles was averaged over the MD trajectories of both the O_2 and CO complexes of the four heme systems. These average "tilts" of the eight systems are listed in Table VII along with the geometrical features listed in Tables II and VI.

Results and Discussion

Reproduction of Model Structures. The overall agreement between the calculated and known geometries, with respect to the features listed in Table II, is very good. The disparities that remain reflect the differences between the stereochemistries of high-spin and low-spin Fe(II) complexes. Closer agreement would result from using two Fe(II) atom types, one for low-spin Fe(II) systems (models a, b, and d) and one for high-spin Fe(II) systems (model c). The largest discrepancies are the differences in the Ct–Np and Fe–Np values. The differences of these two parameters between the experimental systems picket fence (2-MeIm) (high spin) and picket fence (2-MeIm)(O_2) (low spin) are 0.039 and 0.076 Å, respectively. Having two Fe atom types allows one to have a longer r_{eq}(Fe–NP(O)) value for high-spin systems and a shorter r_{eq}(Fe–NP(O)) value for low-spin systems. This will yield both larger Fe–Np and Ct–Np values for the simulated high-spin systems and lower Fe–Np and Ct–Np values for the low-spin systems. However, keeping the number of atom types to a minimum is more in keeping with the overall purpose of force field methods. Using one Fe(II) atom type to describe the four model geometries yields very good agreement and gives us confidence in our force field.

Free Energy Calculations. The trend in the relative CO/O_2 binding affinity of the four representative systems listed in Table IV is reproduced reasonably well with our simplified model. The calculated values correctly predict that the relatively nonpolar 7,7-durene system discriminates in favor of CO over dioxygen when compared to the very polar 5,5-pyridine system. The

Table VII. Values of Geometrical Features as Averages from Trajectories of the O_2 and CO Complexes of Four Hemes Collected at 300 K over 20 ps

	5,5-pyridine(1,5-DCl)		picket fence(2-MeIm)		flat heme(1-MeIm)		7,7-durene(1,5-DCl)	
feature	O_2	CO	O_2	CO	O_2	CO	O_2	CO
Fe–Ct	−0.079 ± 0.066	−0.054 ± 0.102	−0.086 ± 0.094	0.008 ± 0.108	−0.007 ± 0.098	0.064 ± 0.115	−0.020 ± 0.149	0.075 ± 0.105
Fe–core	−0.170 ± 0.097	−0.157 ± 0.104	−0.107 ± 0.110	0.000 ± 0.125	−0.024 ± 0.121	0.060 ± 0.137	0.011 ± 0.148	0.060 ± 0.112
Ct_β–Ct	0.292 ± 0.098	0.284 ± 0.090	0.085 ± 0.052	0.085 ± 0.057	0.102 ± 0.067	0.105 ± 0.065	0.163 ± 0.085	0.097 ± 0.060
Ct–Np	2.022 ± 0.024	2.022 ± 0.019	2.025 ± 0.022	2.019 ± 0.024	2.029 ± 0.018	2.025 ± 0.022	2.056 ± 0.021	2.031 ± 0.021
Fe–Np	2.024 ± 0.024	2.025 ± 0.020	2.028 ± 0.023	2.022 ± 0.024	2.027 ± 0.018	2.029 ± 0.022	2.059 ± 0.021	2.035 ± 0.021
Fe–NB	2.043 ± 0.082	2.067 ± 0.076	2.169 ± 0.076	2.176 ± 0.072	2.075 ± 0.073	2.103 ± 0.071	2.092 ± 0.078	2.086 ± 0.080
Fe–L1	1.788 ± 0.081	1.740 ± 0.092	1.829 ± 0.079	1.773 ± 0.082	1.816 ± 0.077	1.786 ± 0.089	1.864 ± 0.056	1.778 ± 0.086
$-\theta 1$[a]	2.982 ± 4.623	2.374 ± 4.455	1.482 ± 4.502	0.818 ± 4.927	1.628 ± 4.226	0.675 ± 5.093	−2.465 ± 5.217	0.586 ± 4.471
$-\theta 2$	13.264 ± 4.166	13.830 ± 3.969	0.793 ± 4.232	0.856 ± 4.418	1.773 ± 4.040	0.745 ± 4.535	−5.772 ± 3.930	2.904 ± 4.173
$-\theta 3$	0.469 ± 5.003	−1.942 ± 3.834	0.793 ± 4.232	0.856 ± 4.805	1.605 ± 4.213	0.592 ± 5.491	−0.902 ± 3.941	0.262 ± 4.140
$-\theta 4$	13.829 ± 4.686	15.593 ± 3.878	1.063 ± 4.187	0.082 ± 4.674	1.605 ± 4.284	0.735 ± 4.833	−6.426 ± 4.427	2.393 ± 3.965

[a] θi is the angle which pyrrole i "tilts" and is defined by the angle between the mean 24-atom plane and the line from the pyrrole nitrogen to the midpoint of the two β carbons. The straps of the 5,5-pyridine and 7,7-durene systems are attached to pyrroles 2 and 4. The angle is defined as negative for the orientation with the mean plane of the pyrrole group "pointing" to the proximal side.

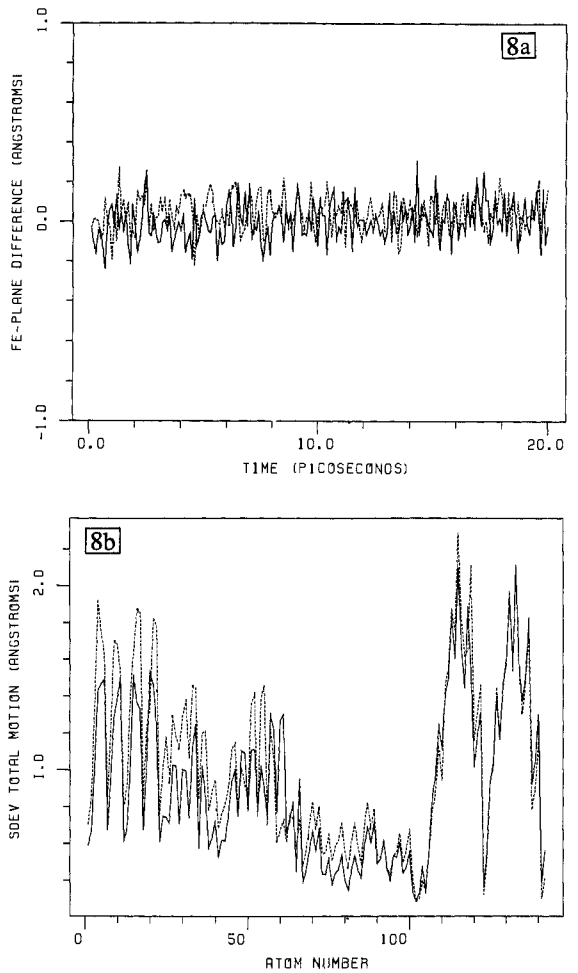

Figure 8. Plots obtained from the MD trajectories of the 7,7-durene system: (—) O_2 complex; (---) CO complex. (a) The Fe–plane distance over 20 ps. (b) The total motion of the individual atoms. Atom numbers 1–22 are the durene cap; 23–64 are the 7-carbon linkages; 65 and 66 are the O_2 or CO ligand; 67–100 are the porphyrin core; 101 is the Fe atom; 102–142 are the 1,5-DCI. Trajectories were collected every 0.1 ps over a total of 20 ps, at 300 K.

$\Delta\Delta G$(calcd) values for these two systems are in very good agreement with the corresponding $\Delta\Delta G$(exptl) values. The $\Delta\Delta G$(exptl) value of the 7,7-durene system is −0.47 kcal/mol while the $\Delta\Delta G$(calcd) value is −1,42 kcal/mol and the $\Delta\Delta G$(exptl) of the 5,5-pyridine system is 4.35 kcal/mol while its $\Delta\Delta G$(calcd) is 5.56 kcal/mol. The former is ~1 kcal too negative while the latter is ~1 kcal too positive. The relative CO/O_2 binding affinity of these three systems can be largely accounted for by considering only the electrostatic and nonbonded interactions and not having to consider the contributions due to the differences in CO–Fe and O_2–Fe bond strengths or differences in solvation. One or both of these factors must be considerably more significant to the picket fence system. That this must be stems from the discrepancy between the $\Delta\Delta G$(calcd) and $\Delta\Delta G$(exptl) values for this system. The $\Delta\Delta G$(calcd) for this system is calculated to favor O_2 over CO by ~5–6 kcal/mol more than the observed preference. Possible reasons for this discrepancy are discussed below.

Differences between the Fe–sixth-ligand bond strengths of the picket fence system and those of the other three cases may stem from the different bases used. The bases used in determining the partition coefficient of the 5,5-pyridine, 7,7-durene, and flat heme systems were 1,5-DCI and 1-MeIm; both of these bases model the "R" state[2a] of hemoglobin. The base used in determining the partition coefficient of the picket fence system is 1,2-MeIm; this base models the "T" state of hemoglobin. The greater steric interaction between the 2-methyl group of this base and the porphyrin core leads to a reduction in the binding affinities of 75 for O_2 and 400 for CO[2a] compared to the corresponding binding affinities of the unstrained "tailed picket fence" system,[2a] This greater destabilization of the CO complex over the O_2 complex leads to a five-fold reduction in the partition coefficient. Correcting for this effect would bring the partition coefficient of the picket fence system *closer* to that of the flat-heme system and would, if anything, make the $\Delta\Delta G$(exptl) value *smaller*. Therefore, the different bases are not contributing to the discrepancy between the $\Delta\Delta G$(exptl) and the $\Delta\Delta G$(calcd) values of the picket fence system.

Collman et al.[2a] suggest that the 5-coordinated "flat" hemes are better solvated than the 5-coordinated picket fence systems, This difference in solvation energy of the two systems decreases upon binding of the sixth ligand. They argue that the 5-coordinated and 6-coordinated picket fence system looks the same to the solvent, whereas the 5-coordinated and 6-coordinated flat heme systems look much different to the solvent. As a result, the flat systems lose more stabilization—due to solvation—in going from the 5-coordinated complex to the 6-coordinated complex than the picket fence systems lose in going from the 5-coordinated complex to the 6-coordinated complex. This difference in solvation between the flat and picket fence systems, with respect to the differential solvation of the respective 5-coordinated and 6-coordinated complexes, lead to a decreased binding affinity of the flat systems relative to the picket fence systems. Although this argument does not suggest that solvation discriminates between the binding of O_2 and CO, it does suggest that the picket fence system could be affected by solvation differently than the other systems and that performing these calculations in a solvent system will yield significant additional information.

To determine how much the charges on the amide groups of the "pickets" were affecting the $\Delta\Delta G$(calcd) values of the picket fence system, a perturbation calculation was run on the picket fence system where charges on the C, O, N, and H of the amide groups were made zero (so as to keep overall neutrality, the

resulting small excess charge was distributed among the α carbon and the ortho-phenyl carbon for each "picket"). This change in charges of the four amide groups had a dramatic affect on the calculated free energy. The so-calculated free-energy, ΔG_4(picket fence), changed from 5.2 to −1.2 kcal. This yields a $\Delta\Delta G$(calcd) of 0.2 kcal/mol, which is much closer to the $\Delta\Delta G$(exptl) value 0.97 kcal/mol. This result suggests that the electrostatic interaction between the bound O_2 ligand and the amide group of the "pickets" is not as dominating an influence in the experimental system as it is in the simulated system. A possible explanation for this is as follows; In the toluene solvent, the amide groups interact favorably with the solvent molecules. When O_2 binds, these amide–solvent interactions are replaced by amide–O_2 interactions. In our calculations, we do not consider the loss of amide–solvent interactions, only the gain in O_2–amide interactions. As recently reported by Levitt and Perutz,[25] aromatic rings can act as hydrogen-bond acceptors from N–H groups. They estimate that this interaction is about half as strong as a normal hydrogen bond, contributing about 3 kcal/mol of stabilizing energy. Thus, our calculations might be expected to exaggerate the strength of O_2 binding. Implicit in this argument is that CO, because of its lower polarity and different geometry, will not interact as strongly with the amide groups and will not be effective in displacing their solute–solvent interactions. For comparison, the same perturbation (performing the $O_2 \rightarrow$ CO perturbation calculation with zero charge on the amide groups) was done with the 5,5-pyridine system. In contrast to the result for the picket fence system, the perturbation calculation on the 5,5-pyridine system—with zero charge on the two amide groups—resulted in a ΔG_4 value of 4.4 ± 0.1 kcal/mol compared with a value of 4.2 ± 0,1 kcal/mol for the 5,5-pyridine system with charges on the two amide linkages. This small difference in ΔG_4 values for the 5,5-pyridine system with and without charges on the amide groups indicates that the amide charges are not as important in the discrimination between the binding of CO and O_2 ligands to the 5,5-pyridine system as they are to the same discrimination in the picket fence system. For the 5,5-pyridine system it is the proximity of the pyridine ring to the ligand binding site that dominates the discrimination between ligands. It appears that the pyridine cap is held in a relatively rigid geometry with its plane in a similar orientation in the presence or absence of the O_2/CO ligand. Thus, solvent would be expected to interact with the pyridine cap similarly in the absence of ligand and in the presence of either the CO or O_2 ligand. This is in contrast to amide groups in the picket fence system, which might be expected to point its N–H groups "outward" to optimally interact with solvent and "inward" to optimally interact with the bound O_2.

There are a few interesting observations that can be drawn from the values listed in Table V. Two of these involve the picket fence system: (1) The nonbonded contribution of the picket fence system is approximately twice that of the flat heme system. (2) The magnitude of electrostatic contribution of the picket fence system is larger that that of the 5,5-pyridine system. To determine how much of these two observations are caused by the fact that different proximal bases were used for the four systems, perturbation calculations were done for the picket fence and flat heme systems using 1,5-DCI as the proximal base. The resulting calculated free energy differences are given in Table VIII along with estimates to the different contributions to these free energy differences. Comparing the estimates to the total NElec contribution of the picket fence systems in Tables V and VIII, where the bases used in the calculations are 2-MeIm and 1,5-DCI, respectively, it is apparent that observation (1) is due almost entirely to the base. This is consistent with the differences in θ_{eq}(NP(O)–Fe–X) values: 93.5° for CO and 91.5° for O_2. In going from O_2 to CO, the Fe proximal base is forced more toward the distal side. When the proximal base is 2-MeIm, this motion toward the distal side increases the interaction between the 2-methyl group of the base and the porphyrin core. When the proximal base is one of the "R-state" bases (1-MeIm or 1,5-DCI), there is no corresponding interaction with the porphyrin core.

Table VIII. Calculated Free Energy Differences of Picket Fence(1,5-DCl) and Flat Heme(1,5-DCl), ΔG_4, as Well as Estimates of the Various Contributions

component	picket fence heme	flat heme heme
EEL[a]	8.407 ± 0.073	2.320 ± 0.009
NONB[b]	−0.003 ± 0.019	−0.033 ± 0.001
14NB[c]	0.199 ± 0.007	0.220 ± 0.006
14EL[d]	−4.424 ± 0.006	−4.407 ± 0.011
BADH[e]	0.316 ± 0.015	0.298 ± 0.010
total Elec[f]	3.983 ± 0.614	−2.087 ± 0.053
total NElec[g]	0.515 ± 0.005	0.485 ± 0.003
ΔG_4(Por$_i$)	4.377 ± 0.118	−1.591 ± 0.051

[a] Electrostatic energy summed over all pairs connected by more than three bonds. [b] van der Waals energy summed over all pairs connected by more than three bonds. [c] van der Waals energy summed over all pairs connected by three bonds. [d] Electrostatic energy summed over all pairs connected by three bonds. [e] Potential energy contribution of all bonds, angles, and dihedral angles that involve one, or both, mutated atoms and at least one atom from a residue that contains no mutating atoms. [f] Sum of EEL and 14NB. [g] Sum of NONB, 14NB, and BADH.

Using the coordinates from the structures of picket fence(2-MeIm)(O_2)[13] and its 1-MeIm analogue[5] and assuming the Fe–CO stereochemistry found for Fe(TPP)(py)(CO),[20] Jameson and Ibers[26] calculated and compared CO and O_2 contacts with atoms of the pickets. They concluded that the close contacts between methyl groups and the terminal oxygen atom, inescapable for the dioxygen ligand, do not occur for their hypothetical CO structure and that these contacts may be an important factor in causing the "tailed-picket" fence system to have an O_2 affinity lower than that found in many hemoglobins. In addition, they pointed out that the CO affinity is higher for the "tailed-picket" fence than for any other system, biological or model, because of the lack of interaction with the bound CO. Contrary to these suggestions, the results from our simplified model indicate that the component of ΔG_4(Por$_i$) due to steric interaction between nonbonded groups (the NONB component in Tables V and VI) is approximately the same for the picket fence and the flat heme systems. This similarity in the nonbonded component between the picket fence and the flat heme systems suggests that even though the contacts between the atoms of the pickets are indeed closer to the bound O_2 ligand than to the bound CO ligand, these contacts contribute very little to the total steric energy of the picket fence systems.

The sign and magnitude of the electrostatic contribution to the free energy difference of the picket fence system did not change in using the base 1,5-DCI. As a result, this contribution must be due to interactions between the sixth ligands and the pickets. Furthermore it suggests that the electrostatic contribution made by the four amide linkages is as great as that made by having a pyridine-3,5-dicarbamide group as close to the binding site as it is in the 5,5-pyridine system. This is consistent with the earlier finding (vide supra) that performing the perturbation calculation on the picket fence system with zero charges on the amide group of the four pickets changed the value of the calculated ΔG_4(Por$_i$) from 5.2 to −1.2 kcal/mol.

A third point that can be brought out from the values in Table V is that the electrostatic contribution of the flat heme and 7,7-durene systems is opposite in sign to that of either the 5,5-pyridine system or the picket fence system. This reflects the much lower polarity of the 7,7-durene system and lack of distal polarity of the flat heme over that of the 5,5-pyridine or picket fence system, this result is consistent with the lower (2 orders of magnitude) dioxygen binding constant of the 7,7-durene system over that of the more polar 7,7-*anthracene cyclophane* heme,[2b] which uses amide linkages instead of the all-hydrocarbon linkages of the 7,7-durene system.

(25) Levitt, M.; Perutz, M. F. *J. Mol. Biol.* **1988**, *201*, 751–4.

(26) Jameson, G. B.; Ibers, J. A. *Comm. Inorg. Chem.* **1983**, *2*, 97–126.

(27) Reichl, L. E. In *A Modern Course in Statistical Physics*; Arnold, E., Ed.; University of Texas Press: Austin, TX, 1980.

In summary, the differences between the calculated values and the experimental values are likely to be attributable to factors not included in the perturbation calculations, solvation and intrinsic energy differences between Fe–CO and Fe–O_2 bonds that differ from one heme system to another.

Molecular Dynamics. The values listed in Table VI under MD average agree with the experimental values except for the Fe–Np and Ct–Np values due possibly to reasons discussed before (vide supra). The very close agreement between simulated and experimental values with respect to the Fe–Ct and Fe–core values is very gratifying and increases our confidence in the force field.

In the Fe–plane position plots of the flat heme (Figure 7a) and picket fence (Figure 6a) systems, the position of the Fe atom is closer to the distal side (more positive in the CO complexes than it is in the O_2 complexes. Inspection of Table VII shows that even though all four systems have the CO complex with a more positive value of Fe–core than the corresponding O_2 complex, the differences between these two vary in the order picket fence(2-MeIm) > flat heme(1-MeIm) > 7,7-durene(1,5-DCI) ≫ 5,5-pyridine-(1,5-DCI).

This difference between the CO and O_2 complexes with respect to the position of the Fe atom reflects the small differences in the equilibrium angles of the two types of systems present in the force field. For the CO complex, the θ_{eq}(Z–Fe–NP(O)) value is 93.5°, while the θ_{eq}(O3–Fe–NP(O)) value of 91.5° is used for the O_2 complexes (see Table III). Having these angles >90° tends to push the Fe atom toward the distal side. Interaction between the proximal base and the porphyrin core tends to pull the Fe atom toward the proximal side. The average position of the Fe atom is a gauge of these two opposing forces. In going from $O_2 \rightarrow$ CO, the Fe–core values of the flat heme and picket fence system increase 0.084 and 0.107 Å, respectively. The difference in these two values reflects the greater interaction between 2-MeIm and the core of the picket fence system than between 1-MeIm and the core of the flat heme system. In going from the $O_2 \rightarrow$ CO the Fe–core values of the 5,5-pyridine and 7,7-durene systems increase 0.013 and 0.059 Å, respectively. Since both of these systems use the same proximal base, 1,5-DCI, the difference between these two values reflects the difference between the interaction of the bound ligands and the distal-side "straps". The difference in Fe–core values for the flat heme systems is ~0.090 Å and is the value obtained in the absence of distal-side steric interaction. The much smaller 0.013-Å difference found for the 5,5-pyridine system reflects the strong interaction between the bound ligands and the cramped 5,5-pyridine strap and must be a stronger interaction than in the 7,7-durene strap. Judging from the differences in the Fe–core values on going from the O_2 systems to the CO systems, the steric interaction with the 5,5-pyridine strap is ~0.059 Å/0.013 Å = 4.5 times greater than it is with the 7,7-durene strap.

This same steric interaction with the 5,5-pyridine strap must be what causes the Fe atom to be 0.060 Å (for the O_2 complex) and 0.160 Å (for the CO complex) more out of the porphyrin plane than it is in the picket fence system. This is even more surprising when one considers that whereas the proximal base used with the picket fence system, 2-MeIm, is used to mimic the "T state" of Hb by pulling the Fe atom out of the porphyrin plane,[13] the proximal base used in the 5,5-pyridine system, 1,5-DCI, is used to mimic the "R" state of Hb[20] which does not have the Fe atom out of the porphyrin plane. Because the average geometrical features found in the MD simulation of the picket fence agree well with those of the experimental system (see Table VI), we feel that this simulated increased displacement of the Fe atom in the 5,5-pyridine system reflects what is occurring in the experimental system. This increased displacement of the Fe atom in the 5,5-pyridine system allows us to make a prediction. This is discussed below.

This increased displacement of the Fe atom from the plane of the simulated 5,5-pyridine system would result in a decreased interaction between the methyl group of a bound 2-MeIm and the porphyrin core of this heme system. As a result, the Fe atom will not be "pulled" out much further by the 2-MeIm base than by the 1,5-DCI base and the properties of 5,5-pyridine(2-MeIm) (an uncharacterized system) will not be very different than the properties of the 5,5-pyridine(1,5-DCI) system.[4] In particular, the ratio of ligand binding constants to heme systems using these "R-state" and "T-state" bases—which reduce as the heme system becomes more encumbered anyway[3]—is predicted to be extremely low for the 5,5-pyridine systems, perhaps the lowest known.

The Ct_β–Ct values of the 5,5-pyridine complexes are 0.20 Å larger than those of the picket fence systems. This value (vide supra) is an indication of the average "tilting" of the four pyrrole groups of the porphyrin cores. The "tilting" of the individual pyrrole groups are listed in Table VII as the $\theta 1$, $\theta 2$, $\theta 3$, and $\theta 4$ parameters. Consistent with the large Ct_β–Ct value, the $\theta 2$ and $\theta 4$ values of the system show that the 5,5-Pyridine system has the largest pyrrole "tilting". The second and fourth pyrrole groups are being forced to "tilt" due to the attachment of the 5,5-pyridine strap. The corresponding pyrrole groups of the 7,7-durene system also show larger tilting angles than the first and third pyrrole groups.

The θi values of the O_2 complex of the 7,7-durene system indicates that these four pyrrole groups are the only ones that "tilt" *toward the distal side*. This result suggests that the Fe–O_2 group of the 7,7-durene system is being "pushed up" toward the distal side more so than in the other seven systems. A possible explanation for this is that the two cyclohexyl groups of the 1,5-DCI proximal base form stabilizing electrostatic interactions with the atoms of the porphyrin core. This electrostatic interaction is not sufficient to cause pyrrole tilting toward the distal side in the other three 1,5-DCI systems because, presumably, it is weaker than the forces keeping the Fe atom toward the proximal side. These are the larger θ_{eq}(Z–Fe–NP(O)) value, relative to the θ_{eq}(O3–Fe–NP(O)) value, and the cramped 5,5-pyridine strap.

The plots of total motion of the individual atoms for the 5,5-pyridine (Figure 5b) and 7,7-durene (Figure 8b) systems show the same general pattern. The two large groups of peaks at the high atom numbers represent the motion due to the free rotation of the 1,5-DCI base about the Fe–NB bond and the chair–chair interconversion of the cyclohexane rings. The lower one-third atom numbers show peaks that represent the motion of the 5,5-pyridine and 7,7-durene straps. The remaining atom numbers show the motion of the atoms of the porphyrin core. The motions of the base and core atoms for both these systems are approximately the same. The motions of the 7,7-durene strap is at least twice that of the motion of the 5,5-pyridine strap. This increased motion of the 7,7-durene system over the 5,5-pyridine system reflects the greater flexibility of the former compared to the latter. The motion of the 5,5-pyridine strap is about the same for both the CO and O_2 ligands. The motion of the 7,7-durene strap has increased motion for the CO complex over that of the O_2 complex. This difference in the motions of the 7,7-durene strap indicates that even though there is great flexibility in having 7-atom linkages, there is still more interaction with a bound CO ligand than with the bound O_2 ligand. This greater interaction between the 7,7-durene strap and the bound CO ligand over the bound O_2 ligand is consistent with the larger Fe–C–O bond angle compared to that in Fe–O–O, ~180° and ~130°, respectively.

The motion plot of the picket fence systems (Figure 6b) shows four repeating peaks starting at about atom number 50. These peaks represent the motions of the four phenylpivalamido "pickets". The motion of the 2-methylimidazole base is shown at atom number 0–12. The rest of the peaks in the motion plot represent the motion of the porphyrin cores. The motion of the CO and O_2 complexes of "picket fence" show no great differences.

The most surprising motion plot is that of the flat heme system, Figure 7b. The O_2 complex shows far greater motion of the porphyrin core than does the CO complex. Only the motion of the Fe (atom number 1) and the base (atom numbers 2–10) are approximately the same for the O_2 and CO complexes. The reason for this increased motion of the O_2 core may be that the atoms of the O_2 core get "pushed around" to a greater extent by the nonbonded interactions with the rotating O_2 ligand than with the CO ligand. The greater nonbonded interactions between the core

atoms and the bound O_2 ligand is consistent with the ~50° smaller Fe–O–O angle than the Fe–C–O angle (vide supra).

Conclusions

The purpose of the present work was to show that force field methods can be successfully applied to investigating properties of heme model systems. We have shown that geometrical properties like the position of the Fe atom with respect to the porphyrin plane and the "tilting" of the pyrrole groups can be reproduced with a simple force field model. This success depended on having a number of available X-ray structures to calibrate our parameters and then using these in other cases. When compared with a variety of data from crystallographic studies, the correspondence between calculations and experiment is very good.

The application of free energy perturbation methods to four heme systems has been quite successful. Relative to the system without an overhead "strap" or a "picket" (designated flat heme in Table IV), the calculations reproduce the relative CO/O_2 preference of the 5,5-pyridine and 7,7-durene hemes. The one exception to this success is the "picket fence" heme, which is calculated to have a much larger binding affinity of O_2 relative to CO than observed. In some sense, this failure is more interesting than the other successes, because with neutralized amide groups, the calculations *do reproduce* the relative affinities very well. Fortunately, there is a good control, the 5,5-pyridine compound with two amide groups. Neutralizing the amide charges in 5,5-pyridine has virtually no effect on its calculated O_2/CO binding free energies. This suggests that, in the absence of O_2 ligand, the N–H groups in the picket fence point outward to interact with the toluene solvent and when O_2 binds, they point in to interact with the O_2. The calculations presented here do not include the solvent effect, so they would be expected and do exaggerate the O_2 affinity of the picket fence system. The predictions from our calculations are that the relative O_2/CO affinity of the picket fence system will increase significantly in aliphatic hydrocarbon solvents which cannot be proton acceptors. NMR studies on the picket fence also could give insight into the structural properties of these compounds in different ligation environments.

The application of molecular dynamics to a number of these iron porphyrins has led to very good agreement with available experiments and to interesting insights into the relative dynamics of different complexes in different ligation states.

The main limitation of these calculations is that solvation effects are not included. The inclusion of solvent effects, particularly the relatively nonpolar solvents used in experimental studies of iron porphyrin systems, would be expected to have a very small effect on the structure and dynamics of these heme systems. Since our calculations focus on the *relative* binding free energy of CO and O_2 for one iron porphyrin system versus another, the relative solvation energies for the ligands should cancel. Since the binding site of O_2 and CO are "well buried", one expects generally small effects on the calculated relative free energies. On the other hand, as noted above, indirect effects, such as the differential interactions of strap N–H groups with aromatic solvents and the O_2 ligand might lead to significant solvent effects on the calculated relative binding free energies. The fact that the "gas-phase" free energy calculations presented here correctly reproduce the relative O_2/CO free energies for two of the three systems relative to flat heme supports our inferences about solvent effects. The "failure" in the one case is very interesting and leads to a prediction.

Further work on modeling O_2/CO affinities in myoglobin, inclusion of solvent, and the modeling of other organometallic systems (vitamin B_{12} models, photosynthesis models, electron-transport models, etc.) show promise for further understanding of the various factors that influence the chemistry in these systems and in the biological systems they model.

Note Added in Proof. While this paper was being refereed, the X-ray structure of a CO–Fe("pocket" porphyrin)(1,2-Me_2Im) system was reported.[28] The structure of this complex is essentially the same as the structure of the CO–Fe(picket fence)(2-MeIm) system we simulated via molecular dynamics, especially the immediate environment at and around the Fe atom. Therefore, the "pocket" system can be compared with our picket fence system. The values for the parameters they report (in angstroms), which are also in our Table VII, are as follows (our values are given in brackets): Fe–C, 1.768 (7) [1.77 (8)]; Fe–NB, 2.079 (5) [2.17 (7)], Fe–Np 1.973 (8) [2.02 (2)]; Fe–core, +0.001 [0.0 (1)]. The agreement is good and is very gratifying, especially with regard to the displacement of the Fe atom from the mean 24-atom plane (Fe–core). Our simulation predicts that the Fe atom will not be displaced at all from the mean plane in spite of the fact that the proximal base (2-MeIm) tends to do just that. The reported structure has verified that prediction and has given even more validity to the force field reported here.

Acknowledgment. M.A.L. has been supported by a postdoctoral fellowship from the National Institute of General Medical Sciences (F32 GM12259). P.A.K. is pleased to acknowledge grant support from the NIH through GM-29072. We acknowledge the use of the UCSF Computer Graphics Laboratory facilities supported by Grant RR-1081 to R. Langridge.

(28) Kim, K.; Fettinger, J.; Sessler, J. L.; Cyr, M.; Hugdahl, J.; Collman, J. P.; Ibers, J. A. *J. Am. Chem. Soc.* **1989**, *111*, 403–405.